CHARACTERIZATION OF INTERPHASE ENVIRONMENTAL DEGRADATION AT ELEVATED TEMPERATURE OF FIBRE-REINFORCED TITANIUM MATRIX COMPOSITES

Theodore E. Matikas

Department of Materials Science and Engineering, University of Ioannina
University Campus, 45110 Ioannina, Greece

Received 16 February 2007; accepted 21 January 2008

ABSTRACT

Fibre reinforced metallic composite materials are being considered for a number of applications because of their attractive mechanical properties as compared to monolithic metallic alloys. An engineered interphase, including the bond strength between the composite's constituents, contributes to a large extent to the improvement of strength and stiffness properties of this class of materials. However, in high temperature applications, where combination of cyclic loading with environmental effects is expected, consideration should be given to interphase degradation, especially in the vicinity of stress risers, such as notches and holes. The applicability of damage tolerance analysis in structural components made of titanium matrix composite materials designed to operate under high temperature environments would depend on the availability of adequate characterization methods for the evaluation of interfacial degradation.

The objective of this paper is to provide a basic understanding of interfacial degradation mechanisms due to oxidation in environmentally exposed titanium-based composites subjected to cyclic stresses. A non-destructive method has been developed enabling high-resolution monitoring of interfacial damage initiation and accumulation as well as surface/subsurface cracking behaviour during interrupted fatigue tests. This non-destructive technique is based on surface acoustic wave propagation in the composites and can detect minute changes in elastic properties of the interfacial region due to elevated temperatures as well as oxygen effects.

Keywords: Metal Matrix Composites, Titanium, Thermo-mechanical Fatigue, Interphase Degradation, Ultrasonic Non-destructive Evaluation, Cracking Behaviour, Environmental Damage, Oxidation

1. INTRODUCTION

Titanium matrix composites (TMCs) reinforced with continuous silicon carbide fibres are good candidates for a number of aerospace applications due to their attractive specific strength and stiffness and high temperature properties. In applications where cyclic loading is expected and where life management is required, consideration must be given to the behaviour of the material in the vicinity of stress risers such as notches and holes, where damage initiation and accumulation is expected. One important damage mode under cyclic loading of fibre reinforced composites is the nucleation and growth of matrix cracks perpendicular to the fibre direction, fully or partially bridged by unbroken fibres [1, 2]. The presence of bridging fibres significantly influences the fatigue crack growth behaviour of the material. This can bring oxygen to the interface region and promote interfacial degradation, leading to eventual failure of the composite. In order to develop a life prediction methodology for these composite systems enabling their full potential application, the mechanism of interfacial degradation at service temperature must be understood and the stress transfer behaviour of the interface should be evaluated.

Interfacial oxidation is one of the most important phenomena that contribute to the material degradation at high temperatures. Oxidation is defined as the chemical reaction between a material and gaseous oxygen to form the oxide material, which can be either solid or gas depending on whether the oxide evaporates. The oxidation of TMC interphase can reduce its strength and consequently reduce the strength and stiffness of the composite structure. It may also potentially introduce other forms of damage such as matrix micro cracking initiated at oxidized interphase region and fibre breakage.

The studies for interphase oxidation in TMCs have been limited despite its importance. Marcus et al. [3] systematically studied the interface of metal matrix composites (Ti-6Al-4V/SiC) including interfacial oxidation. Also, Das et al. [4] extensively studied the

interphase oxidation under elevated temperature using scanning electron microscope. Blatt et al. [5] investigated the effect of thermal/mechanical fatigue loading on interphase oxidation. In their paper, the observation of the stress effect on oxidation rate was first indicated. Jin and Johnson [6] studied the role of oxidation on the thermo-mechanical fatigue of titanium matrix composites and observed reduction in their life due to changes in temperature along with stress that acted as thermal cycle. Osborne et al. [7] examined the effect of temperature and thermal exposure on the interphase behaviour of continuous fibre reinforced TMCs by conducting elevated temperature fibre push-out tests to determine the effect of test temperature on interphase shear properties. Thomas [8] linked the reduced low-cycle fatigue lives of the TMCs to the failure of weak interfaces, particularly due to oxidation damage. Recently, Qin et al. [9] studied the early stage oxidation kinetics in TMCs, and Pardo et al. [10] examined the oxidation behaviour of cast aluminium matrix composites.

The present study focuses on the interphase oxidation mechanisms and the effect of stress level on the interphase oxidation rate. It is desirable that such an investigation will lead to a better understanding of the mechanisms of interphase oxidation as well as stress effect on interphase oxidation. A powerful non-destructive technique is used here to characterize the interphase property. This technique is based in scanning acoustic microscopy which provides crack size information and enables to measure the extent of interfacial degradation and to monitor the process during interrupted fatigue tests. Titanium matrix composite samples used in this work have been subjected to various testing conditions, including room temperature fatigue, isothermal mechanical fatigue, and thermo-mechanical fatigue. Using the experimental characterization data, as well as finite element analysis to obtain the stress distribution, and a model to account for the interfacial oxidation rate actually controlled by oxygen diffusion process, a prediction of interface oxidation under the influence of local stress and temperature was possible.

2. SCANNING SHORT-PULSE ACOUSTIC MICROSCOPY

An innovative technique [11] based on short-pulse acoustic microscopy was used to monitor matrix micro cracking as well as the progression of interphase degradation due to oxidation during interrupted fatigue tests. The most important contrast phenomenon in acoustic microscopy is the presence of Rayleigh surface acoustic waves which are leaking through a coupling medium toward the ultrasonic transducer. The generation and propagation of the leaky Rayleigh waves are modulated by the material properties, thereby making it feasible to image even very subtle changes of local mechanical properties of the testing sample being evaluated.

A highly focused ultrasonic transducer was used in this study. The transducer has a piezoelectric active element situated behind a delay line made of silica crystal oriented such that the 1-1-1 axis is parallel to the direction of sound propagation. The thickness of the active element is suitable to excite ultrasonic signals with a nominal frequency of 50 MHz when an electrical spike voltage is delivered to the piezoelectric element. The ratio of the diameter of the lens to the focal distance of the transducer was 1.25. The focal spot size of the ultrasonic beam was approximately 15 μm when focused on the surface of the TMC sample and the depth of penetration of the surface acoustic waves at 50 MHz was about 140 μm. The principle of operation of a transducer for acoustic microscopy is based on the generation of surface acoustic waves as a direct result of a combination of the high curvature of the focusing lens of the transducer and the defocus of the transducer into the sample. The sensitivity of the ultrasonic signal to surface and subsurface features depends on the degree of defocus and has been well documented in the literature as the V(z) curves [11, 12]. The defocus distance also has another important effect on the surface acoustic wave signal obtained by the transducer; the extent of defocus dictates whether the ultrasonic signal is well separated from the specular reflection or interferes with it. Thus, depending on the defocus, the technique can be used either to map the interference phenomenon in the first layer of subsurface fibres or to map the surface and subsurface features inside the sample. The transducer was raster scanned in a plane parallel to the surface of the sample. The Rayleigh wave amplitude was then digitally recorded and software gated to generate acoustic micrographs.

3. EXPERIMENTS

Specimens were removed during or after testing and evaluated using the scanning acoustic microscopy. All the samples were titanium matrix composites reinforced with a silicon-carbide fibre, commercially designated SCS-6 that has a double pass carbon rich coating. The matrix material was a beta processed titanium alloy, Ti-15Mo-3Nb-3Al-0.2Si (wt.%), with improved environmental resistance at high temperatures. The Ti-15Mo-3Nb-3Al-0.2Si/SCS-6 composites were manufactured using the foil-fibre-foil process.

An isothermal notch fatigue crack growth test was conducted on a 19 mm wide x 0.86 mm thick, four-ply Ti-15Mo-3Nb-3Al-0.2Si/SCS-6 composite sample, with cross-ply lay-up of fibres in the [0/90]S configuration, with an open hole with diameter 3.1 mm at the centre. The specimen was subjected to a maximum stress of 200 MPa applied at 1 Hz along the fibres' direction, while the temperature remained constant at 650°C throughout the test. At this temperature, which is in visco-plastic region for this matrix, the residual stresses should be minimum and their effect should not therefore affect and further damage the composite. However, their redistribution prior to relaxation is expected to cause additional damage; debonding will redistribute the effective stress and make some fibres debond further or break.

Prior to testing, an acoustic micrograph of the specimen was obtained to establish the baseline of initial integrity of the material (Fig. 1). The pre-test image shown in Fig. 1 demonstrates that no interfacial damage was present prior to testing. The fatigue experiment was periodically interrupted and the specimen

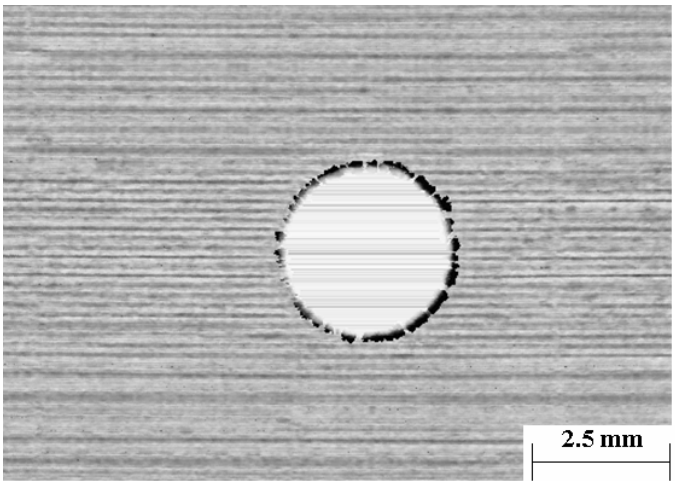

Fig. 1: Acoustic micrograph of Ti-15Mo-3Nb-3Al-0.2Si/SCS-6 composite with [0/90]S cross-ply lay-up of fibres before fatigue testing.

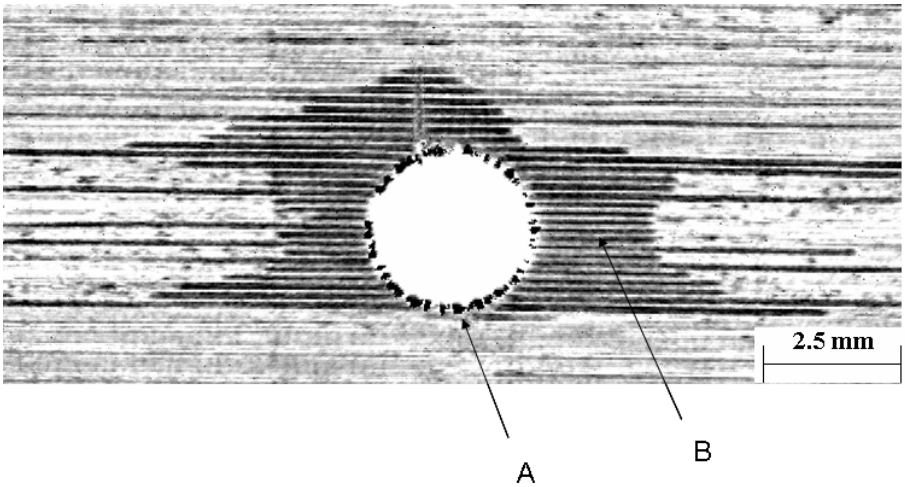

Fig. 2: Acoustic micrograph of Ti-15Mo-3Nb-3Al-0.2Si/SCS-6 composite with [0/90]S cross-ply lay-up of fibres after approximately 43 hours of isothermal (650°C) fatigue test. A. Crack initiation site. B. Interfacial degradation (different pattern than in Fig. 4 due to the [0/90]S vs. unidirectional fibre layout.

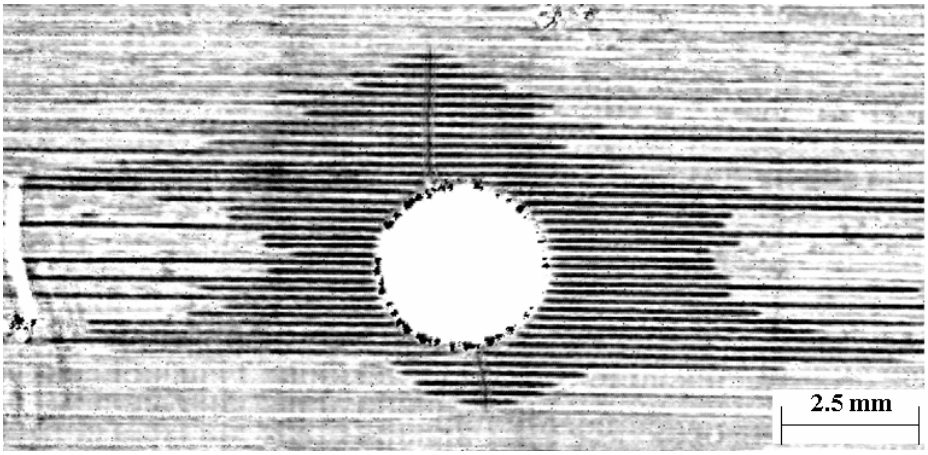

Fig. 3: Acoustic micrograph of Ti-15Mo-3Nb-3Al-0.2Si/SCS-6 composite with [0/90]S cross-ply lay-up of fibres after approximately 70 hours of isothermal (650°C) fatigue test.

was scanned using acoustic microscopy to evaluate the accumulation of damage during the life of the material. The first interruption took place after $1.54x10^5$ cycles or approximately 43 hours at temperature of 650°C (Fig. 2) and was observed that matrix cracks were formed in each side of the hole. Furthermore, it can be clearly observed in Fig. 2 the interfacial damage, indicated by high contrast regions, originated at the top and bottom of the hole, and then preceded away from the hole along the fibres. A second interruption occurred after an additional $9.66x10^4$ cycles were applied for a total of $2.51x10^5$ cycles and total time of 70 hours at the temperature (Fig. 3). In Fig. 3, the cracks on each side of the hole can be clearly seen. The larger crack had grown to a surface length of 2.88 mm from the edge of the hole while the crack on the other side had reached a length of 1.77 mm from the edge of the hole. The region of high contrast (interphase damage) has expanded along the cracks as well as to the left and right of the hole.

The isothermal fatigue behaviour of a second type of Ti-15Mo-3Nb-3Al-0.2Si/SCS-6 sample was investigated. This was a four-ply, unidirectionally reinforced, composite. The specimen was rectangular in shape with a width of 19 mm, length of 150 mm, and had a 4.76 mm diameter hole machined in the centre. The fatigue loading was applied to the specimen in the direction of the fibres at a frequency of 1 Hz and at a maximum applied stress of 350 MPa. Fatigue cracks initiated quickly from the circular hole and propagated until the specimen fractured after $1.82x10^5$ cycles. This corresponded to approximately 50 hours of high temperature exposure during the life of this specimen. After testing, the specimen was evaluated using the acoustic microscopy (Fig. 4). Four cracks initiated around the hole, with one crack on each side of the hole, dominating and eventually leading to failure. One of the non-failure cracks is visible in Fig. 4. A region of high contrast appears along the fibres. The shape of high contrast regions suggests that both the local stresses and the duration of exposure to high temperature environment influence the extent of interfacial damage.

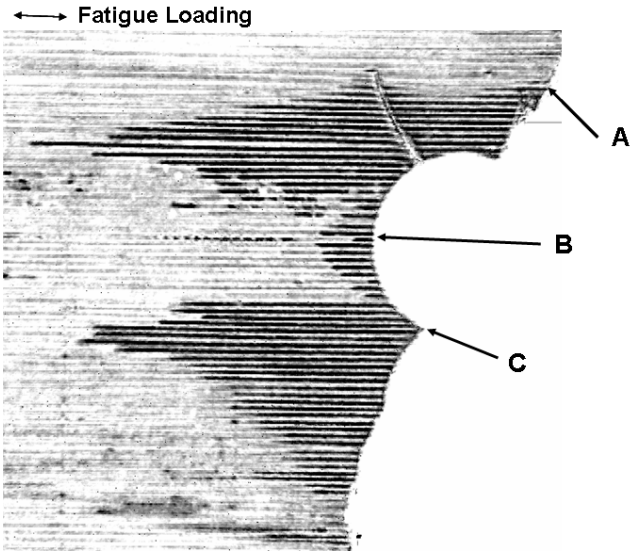

Fig. 4: Acoustic micrograph of Ti-15Mo-3Nb-3Al-0.2Si/SCS-6 composite with unidirectional lay-up of fibres after $1.82x\ 10^5$ cycles of isothermal (650°C) fatigue test: A. Point of accelerated crack growth to failure. B. Interfacial degradation due to compressive stresses. C. Interfacial degradation due to tensile stresses.

4. ANALYSIS

For the TMC composite system the possibility of oxidation exists of all three elements of the composite: titanium matrix, silicon carbide fibres, and fibre/matrix interphase. However, due to the fact that the temperature in the isothermal experiments was limited to 650°C, oxidation of titanium matrix and silicon carbide fibres cannot occur or are not significant [4]. This allows eliminating the possibility of matrix and fibre oxidation, and consequently assuring that the acoustic micrograph presents the image of interphase oxidation alone.

Because of the mismatch of coefficients of thermal expansion (CTE), the residual stresses between fibre and matrix at any below processing temperature always exist. The distribution of oxidation distances around the open hole shown in Figures 2-4 clearly indicate that oxidation distances increase along the matrix crack induced by the notch due to fatigue. This phenomenon is produced by fibre bridging. Unlike the fracture in some polymeric matrix composites, matrix cracking in TMCs does not necessarily suggest the breakage of fibres at the crack surface, especially at early stage of matrix cracking. As a result, it is equivalent to external stresses applied on the fibres at stress free crack surface. The closer to the crack tip, the smaller the applied stress. The oxidation distance varies accordingly. This suggests that stress level significantly affect the oxidation rate. From these figures one can evidently point out the relation between oxidation distance and local stress level. Only exceptions are a few fibres with much higher oxidation distance, which can be attributed to bad consolidation during process.

For a titanium matrix reinforced with SCS-6 fibres, the structure of interphase is composed of several layers including inner and outer carbon rich layers (1.6-2.1 μm), which consumes the majority of thickness (Fig. 5), and a TiC layer (1-1.3 μm) [13]. This carbon rich interphase layers are the result of two sources: the carbon coating originally on the fibre and the oxidation of silicon carbide during process [14]. If the interphase carbon rich layers totally evaporate during oxidation, it will form a gap. When the composite is cooled down to room temperature, the gap is not yet filled by the relief of residual stress caused by mismatch of CTE between fibre and matrix. This finding is supported by the following three arguments. First, acoustic microscopy results in Ref. [5] show much stronger reflective signals at the oxidized interphase. Wave reflection theory supports that this happens only in the presence of an interphase medium with significant reduction in acoustic impedance after the oxidation process. This agrees with the hypothesis of gap formation. Second, in single fibre laser interferometry test using SCS-6 fibre, it has been found that at temperatures around 500°C, the carbon coating is gasified [15]. Third, using simple linear thermal expansion theory one can approximately calculate that the mismatch of CTE will fill the gap by half micron at most, which is far less than the gap created by gasification of carbon layers.

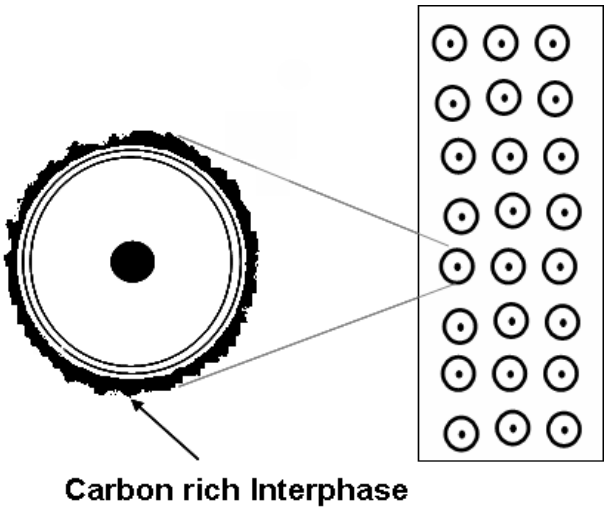

Fig. 5: Titanium matrix composites reinforced with carbon coated SiC fibres have carbon rich interphase region, prone to oxidation at elevated temperatures.

4.1 Stress Analysis

A three dimensional finite element analysis (FEA) was performed to obtain the stress distributions along the open hole using commercially available ANSYS finite element package. In the finite element analysis, the assumption of homogeneous and anisotropic material was made. The material constants of fibre and matrix are listed below:

Table 1: Properties of fibre and matrix materials [19].

	Young's Modulus/ GPa	**CTE**/ x 10^{-6}/°C
Matrix	117.0	4.58
Fibre	413.0	9.94
Interphase	65.1	

The volume fraction of fibre was experimentally determined, as 0.37. The composite mechanical and thermal properties are obtained using Halpin-Tsai equation and Schapery's equation [18], respectively.

The finite element mesh is designed such that not only stress but also the derivative of stress in fibre direction can be obtained. The result of the finite element analysis, the distribution of normal stress in the top ply of fibres along the fibre direction (which is also the loading direction), is shown in Fig. 6.

Since the point of interest is the state of stress in the thin interphase layer, it is suitable that FEA gets into the detail of stresses in the fibre, matrix and interphase, individually. However, this is not always realistic due to the limited computational resources. This issue can be resolved by using the assumption of anisotropic, but homogeneous, material for each of the composite plies treated by FEA. After the stress state is obtained, one can proceed to determine the stress state at the interphase. It is certainly not the most accurate assessment, but a simple model can be utilized to maximize the accuracy.

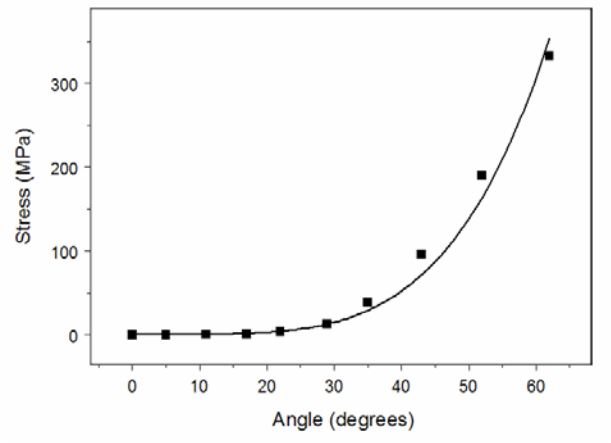

Fig. 6: Distribution of stress around the hole along the fibre direction.

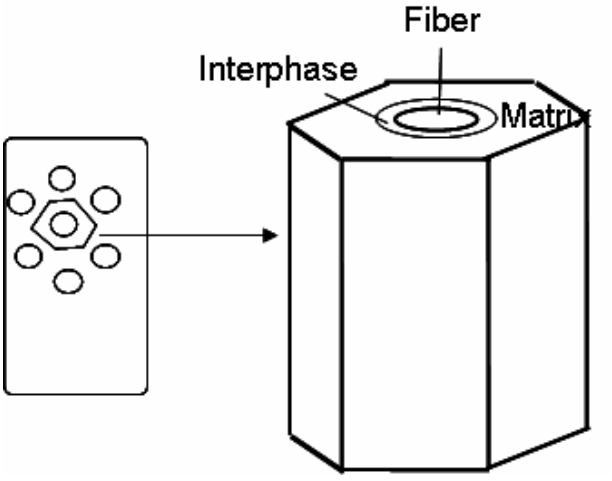

Fig. 7: Schematic of prism model for interphase stress.

A unit of prism of matrix with a fibre at the centre (see Fig. 7) can be considered. The side faces of the prism define the dividing plane with other single fibre units. It is assumed that the unit is small enough so that the deformation on the unit is uniform. According to the assumption, stress equilibrium and strain continuity exist, as follows:

$$\sigma_y A = \sigma_f A_f + \sigma_m A_m + \sigma_i A_f \quad (1a)$$

$$\sigma_y = \sigma_f V_f + \sigma_m \left(1 - V_f\right) \quad (1b)$$

$$\frac{\sigma_f}{E_f} = \frac{\sigma_m}{E_m} = \frac{\sigma_i}{E_i} \quad (2)$$

where, A and E are the prism cross-section area and Young's modulus; f, m, i denote fibre, matrix, and interphase, respectively; and Vf is the fibre volume fraction. Because the thickness of the interphase is relatively small, the last term in Eq. 1a can be ignored. Af/A is further let to be equal to the volume fraction 0.37. Using Young's moduli of fibre, matrix and interphase as per Table 1 (assuming Poisson's ratio 0.3 and interphase thickness 3 mm), the normal stress on the interphase was found to be approximately 29% of the local stress. It should be finally noted that as long as oxidation occurs the original stress state is no longer valid. The further the oxidation propagates the poorer the representation of the original stress state.

4.2 Diffusion Model

As observed in Ref. [5], the only oxygen source is from the fibre cut-off surface along the open hole or the notch. Therefore, at the temperature range of the experiment, the oxidation rate is actually controlled by the oxygen diffusion into the interphase [3]. There are many factors that affect the interphase diffusion rate, including temperature, exposure time, thermal/mechanical fatigue loading, and local stress level, etc. it is reported that the diffusion at interphase can be much higher than the bulk diffusion for the same

material [3]. Using the assumptions that the interphase is one-dimensional, half infinite medium and undergoes the diffusion of a constant concentration of oxygen, the theoretical model for stress assisted diffusion [16, 17] has been developed.

Fick's law of diffusion is modified to consider the stress effect.

$$\frac{\partial C}{\partial t} = D\left[\frac{\partial^2 C}{\partial x^2} - \frac{F}{kT}\frac{\partial C}{\partial x}\right] \tag{3}$$

where, C is the oxygen solute concentration, D the diffusion coefficient, F the stress (diffusive force), k Boltzman's constant, and T the temperature in degrees Kelvin. x and t denote the distance and time, respectively.

Let $D\frac{F}{kT} = a$, then

$$\frac{\partial C}{\partial t} = D\frac{\partial^2 C}{\partial x^2} - a\frac{\partial C}{\partial x} \tag{4}$$

The boundary and initial conditions are:

$$x = 0, \quad C = C_o \tag{5a}$$

$$x \to \infty, \quad C \to 0 \tag{5b}$$

$$t \le 0, \quad C = 0 \ (for\ x > 0) \tag{5c}$$

Laplace transform is then used to solve the differential equation from Fick's law for given solute concentration which will cause oxidation.

$$\int_0^\infty e^{-pt}\left[D\frac{\partial^2 C}{\partial x^2} - Q\frac{\partial C}{\partial x}\right]dt - \int_0^\infty e^{-pt}\frac{\partial C}{\partial t}dt = 0 \tag{6}$$

Integrating by parts,

$$\int_0^\infty e^{-pt}\frac{\partial C}{\partial t}dt = \left[Ce^{-pt}\right]_0^\infty + p\int_0^\infty Ce^{-pt}dt = p\bar{C} \tag{7}$$

Then we have:

$$D\frac{\partial^2 \bar{C}}{\partial x^2} - a\frac{\partial \bar{C}}{\partial x} = p\bar{C} \tag{8}$$

By treating the boundary condition (Eq. 5a), we obtain $\bar{C} = \frac{C_o}{p}$. (4)

Hence, the Laplace transform reduces the partial Eq. (4) to an ordinary differential equation.

$$D\bar{C}'' - a\bar{C}' - p\bar{C} = 0 \tag{9}$$

with the solution,

$$\bar{C} = \bar{A}_1 e^{\left[\frac{a-\sqrt{a^2+4Dp}}{2D}\right]x} + \bar{A}_2 e^{\left[\frac{a+\sqrt{a^2+4Dp}}{2D}\right]x} \tag{10}$$

Since $x \to \infty, \quad C \to 0$, which leads to $\bar{A}_2 = 0$ (11a)

$$x = 0, \quad \bar{C} = \frac{C_o}{p}, \text{ which leads to } \bar{A}_1 = \frac{C_o}{p} \tag{11b}$$

Therefore,

$$\bar{C} = \frac{C_o}{p} e^{\left[\frac{a-\sqrt{a^2+4Dp}}{2D}\right]x} \tag{12}$$

Finally,

$$C = \frac{C_o}{2}\left\{erfc\left(\frac{x-at}{2\sqrt{Dt}}\right) + e^{\frac{ax}{2D}}erfc\left(\frac{x+at}{2\sqrt{Dt}}\right)\right\} \tag{13}$$

Now it is possible to obtain the diffusion propagation rate for given concentration, and consequently the oxidation propagation rate for the solute concentration, considering oxide gasification. When x is small compared to (at), the first term of Eq. (13) is much larger than the second term. Therefore, for given concentration, C^*, which will lead to oxidation we obtain,

$$C^* = \frac{C_o}{2} erfc\left(\frac{X-at}{2\sqrt{Dt}}\right) \tag{14}$$

with

$$X = 2\sqrt{Dt}\ f\left(\frac{2C^*}{C_o}\right) + at \tag{15}$$

where, X, denotes the oxidation distance, and f is the inverse of the error function complement, erfc.

Equation (15) shows that the diffusion propagation rate is linear combination of two terms. The first term is proportionate to the square root of time and coincides with the diffusion model without stress effect. The second term is proportionate to time and is solely contributed by local stresses.

However, taking into account gasification of oxide, one can conclude that oxidation occurs earlier than can be detected with acoustic microscopy. At the stage that oxidation is observed, the interphase has been close to being gasified. If oxidation is ignored before it can be observed by acoustic microscopy, and considering that oxidation is complete after the observation is made, one could move the reference frame with the oxidation demarcation point. Therefore, after oxidation occurs, it becomes a simple moving boundary problem. With the assumption of half infinite diffusion medium, the oxidation rate will be defined as X', a constant:

$$X' = \frac{f\left(\frac{2C^*}{C_o}\right)\sqrt{D}}{\sqrt{t}} + a \qquad (16)$$

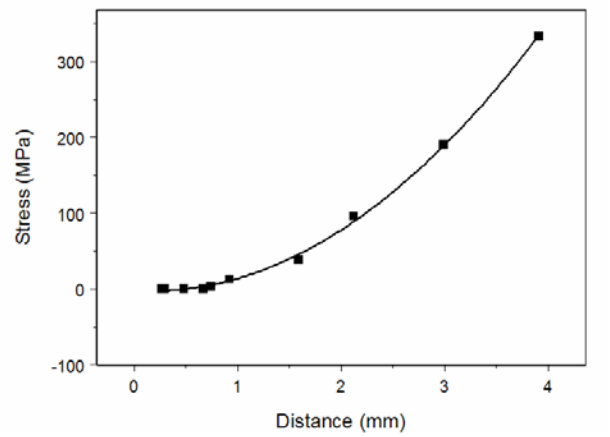

Fig. 9: Oxidation distance vs. normal stress in the top ply of fibres along the fibre direction, estimated using finite elements analysis.

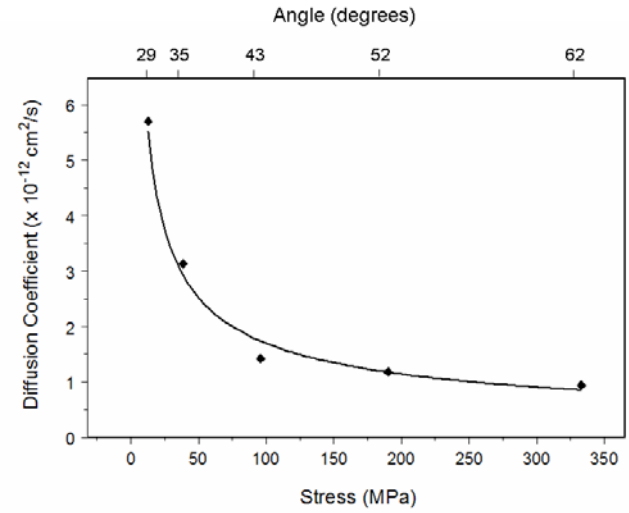

Fig. 10: Diffusion coefficient of interphase oxidation as a function of normal stress and angle around the hole of the sample.

The oxidation distance vs. time finally becomes,

$$X_o = \left[\frac{f\left(\frac{2C^*}{C_o}\right)\sqrt{D}}{\sqrt{t_o}} + a\right] t \qquad (17)$$

where, t_o is the time when oxidation is first observed.

X_o is the combination of two terms: the primary oxidation distance and excessive oxidation distance. The first term is the original oxidation and the second term is the contribution of stress.

5. RESULTS

Based on the acoustic micrographs showing interfacial degradation due to mechanical fatigue of the same sample at 650°C for 43 hours and 70 hours (Figs. 2 and 3), respectively, the oxidation distance around the hole was measured in top ply of fibres (Fig. 8). It is observed that the oxidation distance increases with the angle around the hole. This is expected since the stress also rises for higher angles.

Fig. 9 shows the oxidation distance as a function of normal stress in the top ply of fibres along the fibre direction, estimated using finite elements analysis. It becomes evident that the oxidation distance increases with the raise of stress.

Based on the developed diffusion model, the diffusion coefficient was calculated from experimental data on the extent of interphase oxidation, as well as on finite element estimation of stress distribution. Fig. 10 shows the diffusion coefficient as a function of stress and angle around the hole of the sample. It can be observed from the Figure that the diffusion coefficient of interfacial oxidation decreases with the increase of angle (and stress). However, this coefficient is expected to be a constant at given temperature and concentration. The explanation for this apparent contradiction is that stress is relieved after oxidation occurs, since the failure of interphase will reduce the contribution of fibres to the distribution of stresses. More the interphase is gasified, more stress will be relieved. Nevertheless, in finite element analysis for stress estimation no stress relief mechanism is considered. High angle regions are thus expected to have lower stress concentration than the one pre-

dicted in the finite element analysis. It is reasonable therefore to argue that the diffusion coefficients obtained at lower angles around the hole are more accurate. Based on this reasoning, the diffusion coefficient of interphase oxidation was estimated to be about 5×10^{-12} cm^2/s.

6. CONCLUSIONS

The purpose of this study is to have a better understanding of the mechanisms of interphase oxidation and the role played by local stress on interphase oxidation. Using acoustic microscopy, experimental results on the extent of interphase oxidation have been obtained. Using finite element analysis, the stress distribution has been estimated. Finally, using the developed diffusion model, the interphase oxidation under the influence of local stress was predicted and the diffusion coefficient of interfacial oxidation was determined. It is demonstrated that both the time of exposure of the interface in oxygen atmosphere, as well as the level of stresses, significantly affect the oxidation rate.

It is interesting that the acoustic microscopy images showed a clear demarcation between oxidized or unoxidized interphase. The top ply of the samples used was etched off to observe the interphase degradation. It was found that the transition between carbon rich interphase and gasified interphase is abrupt. In addition, this transition precisely corresponds to the transition observed using acoustic microscopy. This not only confirms the results obtained using acoustic microscopy, but also illustrates the usefulness of acoustic microscopy technique in interphase oxidation research. In fact, acoustic microscopy is a powerful non-destructive tool that enables in situ monitoring of interphase oxidation during interrupted tests.

Generally speaking, interphase oxidation is very complex problem. The case studied in this work can be considered as a simple one, since at the temperature range of the oxidation test the oxidation of fibre and matrix is insignificant. Further, there are assumptions used in the model that may not fully represent the real situation under different circumstances. Therefore, more studies are necessary in order to have a complete understanding of interphase oxidation mechanisms.

References:

1. **Waterbury M.C., Karpur P., Matikas T.E., Krishnamurthy S., Miracle D.B.,** "In situ observation of the single-fibre fragmentation process in metal-matrix composites by ultrasonic imaging", *Composites Science and Technology,* **52**/2 (1994), 261-266.
2. **Majumdar B.S., Matikas T.E., Miracle D.B.,** "Experiments and analysis of fibre fragmentation in single and multiple-fibre SiC/Ti-6AI-4V metal matrix composites", *Composites Part B: Engineering*, **29**(2) (1998), 131-145.
3. **Marcus, H. L.,** "Titanium Matrix/Continuous Fibre Composite Interface Interactions and Their Influence on Mechanical Properties", *Technical Report AFOSR-TR-84-0812*, August 1984.
4. **Das, G. and Vahldiek, F. W.,** "Effects of Elevated Temperature Oxidation on the Reaction Zone of a SiC Fibre-Reinforced Ti3Al-11Nb Composite", Interfaces in Metal-Ceramics Composites, Ed. R. Y. Lin, R. J. Arsenault, G. P. Martins and S. G. Fishman, The Minerals, Metals & Materials Society, 1989.
5. **Blatt, D., Karpur, P., Matikas, T. E., Blodgett, M. P. and Stubbs, D. A.,** "Elevated Temperature Degradation and Damage Mechanisms of Titanium Based Metal Matrix Composites with SCS-6 Fibres", *Scipta Metallurgica et Materialia,* **29** (1993), 851-856.
6. **Jin, O. and Johnson, W. S.,** "Role of Oxidation on the Thermo-mechanical Fatigue of Timetal 21S Matrix Composites", *ASTM Special Technical Publication,* 1371 (2000), 204-222.
7. **Osborne, D., Chandra, N. and Ghonem, H.,** "Interphase Behaviour of Titanium Matrix Composites at Elevated Temperature", *Composites Part A: Applied Science and Manufacturing,* **32**/3-4 (2001), 545-553.
8. **Thomas, M. P.,** "Effect of Matrix and Fibre Type on Low Cycle Fatigue of [90]8 Sigma Fibre Reinforced Titanium Matrix Composite", Composites Science and Technology, **63**/5 (2003), 587-595.
9. **Qin, Show, Y., Lu, Show, W., Xu, Show, D., Zhang, Show, D.,** "High-temperature OM Investigation of the Early Stage of (TiC+TiB)/Ti Oxidation", *Journal of Materials Science,* **40**/3 (2005), 687-692.
10. **Pardo, A., Merino, M. C., Arrabal, R., Feliu Jr., S. and Viejo, F.,** "Oxidation behaviour of cast aluminium matrix composites with Ce surface coatings", *Corrosion Science,* **49**/7, (2007), 3118-3133.
11. **Matikas, T. E.,** "Quantitative Short-Pulse Acoustic

Microscopy and Application to Materials Characterization", Microscopy and Microanalysis, 6 (2000), 59-67.

12. **Liang, K. K., Kino, G. S. and Khuri-Yakub, B. T.,** "Material Characterization by the Inversion of V(z)", IEEE Transactions on Sonics and Ultrasonics, SU-32 (1985), 213-224.
13. **Lawrence, C. W., Briggs, G. A. D. and Scruby, C. B.,** "Acoustic Microscopy of Ceramic-Fibre Composites, Part III Metal-Matrix Composites," **Journal of Materials Science**, **28** (1993).
14. **Qi, G., Spear, K. E. and Pantano, C. G.,** "Carbon-Layer Formation at Silicon-Carbide-Glass Interfaces," *Materials Science and Engineering*, A162 (1993).
15. **Kent, R.,** private communication.
16. **Shewmon, P.,** "Diffusion in Solids", Publication of The Minerals, Metals and Materials Society, 1989.
17. **Crank, J.,** "The Mathematics of Diffusion", Oxford Science Publications, Oxford, 1989.
18. **Chawla, K. K.,** "Composite Materials - Science and Engineering", *Springer-Verlag*, New York, 1987.
19. **Matikas, T. E. and Karpur, P.,** "Micro-mechanics Approach to Characterize Interfaces in Metal and Ceramic Matrix Composites", D. O. Thompson and D. E. Chimenti, Eds., Review of Progress in Quantitative Nondestructive Evaluation, **13B**, 1477-1484, (Plenum, New York, 1994).